



# Self-assembly of isotropic colloids into colloidal strings, Bernal spiral-like, and tubular clusters†

 Yong Guo, \*<sup>a</sup> Bas G. P. van Ravensteijn \*<sup>b</sup> and Willem K. Kegels<sup>c</sup>

 Cite this: *Chem. Commun.*, 2020, 56, 6309

 Received 5th February 2020,  
Accepted 28th April 2020

DOI: 10.1039/d0cc00948b

rsc.li/chemcomm

**We report the (spontaneous) formation of colloidal strings, Bernal spiral-like, and tubular clusters comprising spherical, isotropically functionalized colloidal particles in an aqueous environment. The formation of colloidal strings and Bernal spiral-like clusters is guided by an interplay between short-ranged hydrophobic attraction and relatively longer-ranged electrostatic repulsion acting between the colloids. When a dispersion of these colloids is densified via centrifugation, well-defined tubular aggregates were observed.**

Assembling colloidal building blocks in desired superstructures is not only a powerful route towards the development of functional materials with tailored photonic, sensing and catalytic properties, but also provides fundamental insight into, for example, the phase behavior of atoms and molecules.<sup>1</sup> A common strategy for assembling colloids is to reverse-engineer the required building blocks for a target assembly relying on geometric arguments. Typically, anisotropic or so-called ‘patchy particles’ are the building blocks of choice. The use of patchy particles, which contain areas (patches) attractive or repulsive toward patches present on other particles, opens up avenues to a wide variety of superstructures since bond directionality and valence can be imprinted within the building blocks by the number and relative orientation of the patches. Experimentally, patchy particles were successfully assembled into colloidal micelles,<sup>2</sup> microcapsules,<sup>3</sup> free-standing monolayers,<sup>4</sup> Kagome lattices,<sup>5</sup> supra-colloidal helices,<sup>6</sup> and ‘colloidal molecules’.<sup>7</sup>

Despite the great synthetic advances in colloid chemistry, preparation of (anisotropic) multi-patch particles in sufficient yield and purity remains a great challenge, hampering structural variation of the accessible assemblies. To circumvent

these practical limitations, there is a push towards using (synthetically) less demanding systems such as spherical colloids which are isotropic in both their shape and surface functionality for the fabrication of aforementioned complex assemblies. In these systems, the directionality or symmetry breaking of the assembly process is not governed by geometry, but relies on, for example, the asymmetric re-arrangement of surface-grafted ligands<sup>8</sup> or exploiting intrinsically anisotropic dipolar interactions between individual colloids.<sup>9</sup>

Alternatively, theoretical and simulation studies have shown that (equilibrium) finite-sized cluster phases comprised of aggregates with well-defined dimensions and geometries are accessible by delicately tuning the balance between short-range attractions and long-range repulsions acting between the individual particles.<sup>10–12</sup> The cluster shape and size was found to sensitively depend on the balance between the competing inter-particle forces. For example, when the cluster diameter exceeds the Debye screening length of the long-range repulsion, and simultaneously the magnitude of the long-range repulsion is sufficiently large, elongated clusters were found. In agreement with these earlier simulation results, a recent study using methods of inverse inter-particle potential design, revealed that isotropic pair potentials consisting of a short-range attraction and a longer-range repulsion can promote the formation of elongated clusters including strings and Bernal spirals.<sup>11b</sup> Experimentally, these findings were reproduced in a colloidal system where electrostatic repulsion was complemented with a short-range depletion-induced attraction in an organic solvent.<sup>12a</sup> Bernal spiral-like structures were observed in this particular case. The Bernal spirals consist of three twisting particle strands in which each particle is in contact with six neighboring particles.<sup>6</sup>

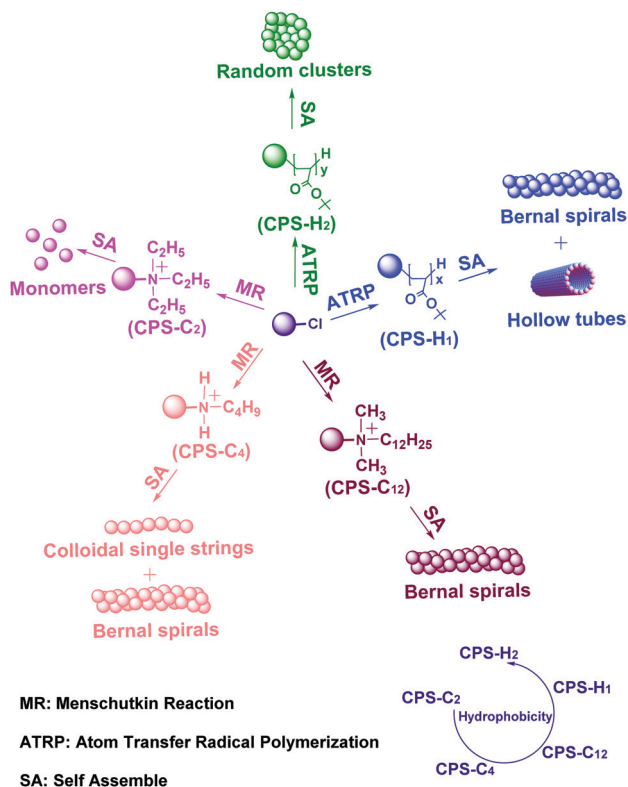
Herein, we expand the set of experimental systems capable of forming elongated clusters by combining a short-ranged hydrophobic attraction and a relatively longer-ranged electrostatic repulsion acting between the building blocks in an aqueous environment. The hydrophobic attractions are accomplished by grafting hydrophobic surfaces layers onto charge-stabilized particles.

<sup>a</sup> School of Medicine, Hangzhou Normal University, Hangzhou 311121, People's Republic of China. E-mail: yongguo1987@gmail.com

<sup>b</sup> Institute for Complex Molecular Systems, Eindhoven University of Technology, 5600 MD Eindhoven, The Netherlands. E-mail: b.g.p.v.ravensteijn@tue.nl

<sup>c</sup> Van't Hoff Laboratory for Physical and Colloid Chemistry, Debye Institute for NanoMaterials Science, Utrecht University, 3584 CH Utrecht, The Netherlands

† Electronic supplementary information (ESI) available. See DOI: 10.1039/d0cc00948b



**Scheme 1** Schematic illustration of the preparation of charge-stabilized colloids grafted with hydrophobic surface layers and their corresponding self-assembled structures.

Under the right conditions, *i.e.*, the appropriate balance between the repulsive electrostatic contribution and attractive hydrophobic contribution, elongated assemblies were formed. Intriguingly, besides the previously observed Bernal spiral-like assemblies, two additional cluster morphologies were experimentally identified, namely colloidal strings with the width of a single particle diameter, and hollow tubular structures. Considering that the combination of hydrophobic attractions and electrostatic repulsions is extensively encountered in biological systems, our findings might shed light on the mechanisms underlying spontaneous anisotropic structure formation observed in protein systems.<sup>13</sup>

Hydrophobic entities were introduced on the surface of charged colloids, *via* a Menschutkin reaction (Scheme 1).<sup>14</sup> Negatively charged colloids surface-functionalized with benzyl chloride moieties (CPS-Cl with a radius of 155 nm and a zeta ( $\zeta$ ) potential of  $-38$  mV) were used for this purpose.<sup>15</sup> The CPS-Cl particles were synthesized by co-polymerizing vinylbenzyl chloride and divinylbenzene on the surface of cross-linked polystyrene particles by seeded emulsion polymerization. The negative surface charge of CPS-Cl is provided by sulfate and sulfonate moieties that originate from the applied initiator system. The pendant benzyl chlorides were reacted with a variety of aliphatic amines, allowing for the attachment of relatively short hydrophobic hydrocarbon segments ( $C_2$ – $C_{12}$ ) onto the CPS-Cl surface. The grafting of the aliphatic chains is accompanied by the formation of (permanently) charged amines.<sup>14</sup> The net charge of the colloids is therefore set by the sum of the initially present negative charges

and the newly introduced positively charged amine derivatives. This procedure enables us to tune the surface/ $\zeta$  potential and surface hydrophobicity by controlling the functionalization time and selected aliphatic amine. Therefore, this system enables a systematic investigation on the influence of the strength of the hydrophobic attraction and electrostatic repulsion on colloidal aggregation behavior. After modification, the hydrophobized colloids were washed and dispersed in pure water. Subsequently, the dispersions (volume fraction  $\approx 0.5\%$ ) were equilibrated for one week. After spontaneous particle sedimentation, the samples were gently redispersed by manual shaking and the morphology of the assembled structures was assessed.

Fig. 1 summarizes the clustering behavior of colloids grafted as a function of time during a surface modification with *N,N*-dimethyldodecylamine ( $C_{12}$ ). In the early stages of the functionalization procedure, the conversion of the Menschutkin reaction is low, yielding strongly negatively charged particles ( $\zeta = -30$  mV) with a low surface density of grafted hydrophobic amines. The strongly dominating electrostatic repulsion ensures that the colloids are well-dispersed (Fig. 1b), no persisting clusters are formed. With the Menschutkin reaction proceeding, an increasing number of positive charges are generated on the colloidal surface. The accompanied decrease in net charge

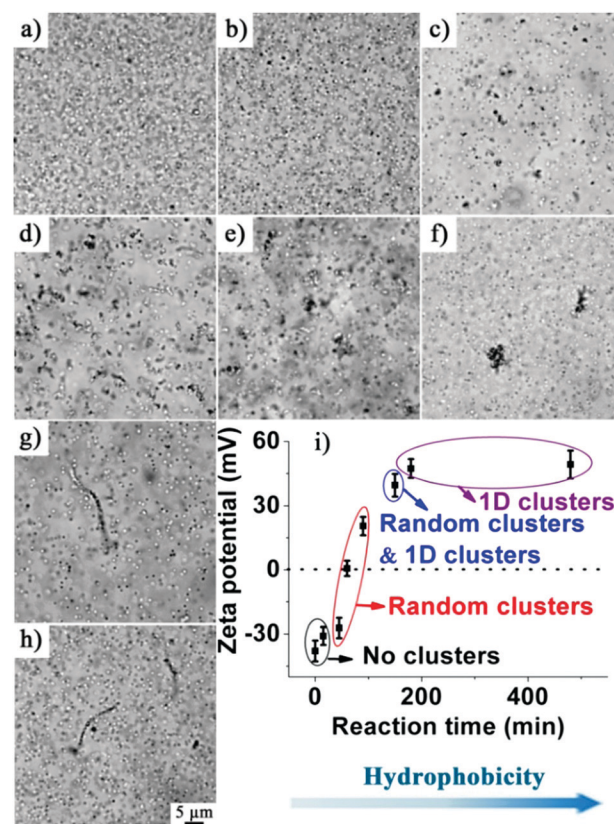


**Fig. 1** Optical micrographs of assemblies comprising CPS- $C_{12}$  during functionalization with *N,N*-dimethyldodecylamine. Aliquots were withdrawn after (a) 0, (b) 5, (c) 45, (d) 60, (e) 90, (f) 150, (g) 180, and (h) 480 min. (i) Zeta ( $\zeta$ ) potential of CPS- $C_{12}$  as a function of reaction time. The clustering behavior of CPS- $C_{12}$  during amine grafting is classified according to microscopy observations. Scale bar: 5  $\mu$ m for all images.

density is evident from the  $\zeta$  potential which approaches 0 mV after approximately 60 min. At this point, the electrostatic repulsion is minimal. Simultaneously, the hydrophobic attraction constantly gains in strength since more hydrophobic entities are grafted onto the colloidal surface. Under these conditions, the electrostatic repulsion is too weak to overcome the hydrophobic attraction, resulting in the formation of random aggregates (Fig. 1c–f, i). As the surface density of grafted amines continues to increase, the sign of the  $\zeta$  potential reverses and the magnitude of the electrostatic repulsion increases again, leading to the formation of elongated aggregates (Fig. 1g and h).

As attractive van der Waals forces are not dominant in this system,<sup>14</sup> the assembly is primarily driven by hydrophobic attractions caused by the grafted aliphatic amines (ESI,† S2).

After identifying the experimental window in which elongated aggregates were formed, we set out to probe the effect of the length of the hydrophobic alkyl chains grafted to the colloids on their assembly behavior. Relying on the aforementioned Menschutkin reaction, amines with varying aliphatic alkyl tails were grafted onto CPS-Cl (number of carbons = 2 (CPS-C<sub>2</sub>), 4 (CPS-C<sub>4</sub>) or 12 (CPS-C<sub>12</sub>), Scheme 1). Regardless of the hydrophobic tail length of the employed amines, colloidal systems with similar  $\zeta$  potentials ( $\sim 45$  mV) were obtained, implying that the grafting densities and therefore the electrostatic repulsion between the amine modified colloids, are comparable. The colloids have no propensity to cluster and remain well dispersed when short alkyl chains were immobilized onto the colloidal surface ( $n < 4$ , Fig. 2a and b). However, elongated aggregates were observed for both CPS-C<sub>4</sub> (Fig. 2c) and CPS-C<sub>12</sub> (Fig. 2d), highlighting that small variations in the hydrophobic contribution to the inter-particle potentials have a distinct influence on

the clustering behavior. Intriguingly, CPS-C<sub>12</sub> assembled exclusively into Bernal spiral-like structures with a fraction of 10 per 10<sup>8</sup> particles (Scheme 1 and Fig. 2h), while for CPS-C<sub>4</sub>, Bernal spirals coexist with colloidal strings, which have a width of only one particle diameter (Scheme 1 and Fig. 2c, g). The fractions of Bernal spiral-like structures and strings of CPS-C<sub>4</sub> are approximately 5 and 10 per 10<sup>8</sup> particles, respectively.

To further investigate the influence of surface hydrophobicity on the accessible cluster morphologies, a surface confined Atom Transfer Radical Polymerization (ATRP) was employed. This procedure allows for grafting homogeneous hydrophobic brushes with a greater brush height, *i.e.*, thicker hydrophobic surface layers (Scheme 1 and ESI,† S3). The benzyl chloride moieties on the particles functioned as polymerization initiators and therefore effectively act as grafting point for a single polymer chain. Poly(*t*-butyl acrylate) (p(*t*BA)) was grafted from CPS-Cl to yield CPS-H<sub>1</sub> with a highly hydrophobic surface of approximately 6 nm thickness as determined by TEM. As the overall hydrophobicity is the key parameter in determining the assembly behavior, chemical differences between the p(*t*BA) brushes and the previously used amines are hypothesized to be irrelevant here. Infrared (IR) spectroscopy confirmed the presence of the hydrophobic polymer layer. The relatively intense p(*t*BA)-related IR signal implies that the hydrophobic surface layer of the CPS-H<sub>1</sub> is thicker than that of the amine-derived monolayers. In the latter case, the introduced amines proved to be undetectable and the recorded IR spectrum was completely dominated by the polystyrene bulk of the particles (Fig. S2, ESI†). Furthermore, to facilitate the direct comparison with the aliphatic amine functionalized CPS-C<sub>*n*</sub> ( $n = 2, 4, 12$ ), the polymer grafting was performed in DMF. As reported before, a fraction of the benzyl chlorides reacts with DMF (or its degradation products) to generate permanently positively charged amines to the surface, resulting in a final  $\zeta$  potential of 30 mV.<sup>14</sup> Analyzing the clustering behavior of CPS-H<sub>1</sub> in pure water revealed that Bernal spiral-like structures were formed exclusively. The results are consistent with simulations of Banerjee *et al.* where the formation of short particle strings and Bernal spirals was observed *via* systematic variation of short-range attractions and longer-range repulsions.<sup>11b</sup> Further increasing the surface hydrophobicity by grafting longer polymer brushes (CPS-H<sub>2</sub>) yielded unstructured aggregates (Fig. 2f).

Finally, the delicate balance between competing contributions to the interparticle potential required to stabilize anisotropic clusters was confirmed by the addition of salt. Lowering the range and strength of the electrostatic repulsion resulted in a morphological transition from elongated to compact spherical aggregates (Fig. S3, ESI†).

For the elongated structures to form, fairly high particle concentrations were required. The low concentration of aggregates compared to single particles suggests that weak attractions are driving the assembly. To accelerate and promote the self-assembly process and potentially increase the yield of elongated clusters, the aforementioned samples were delicately centrifuged (2100g, 2 h), followed by gently redispersing the sedimented particles/clusters. For CPS-C<sub>2</sub>, CPS-C<sub>4</sub>, CPS-C<sub>12</sub> and

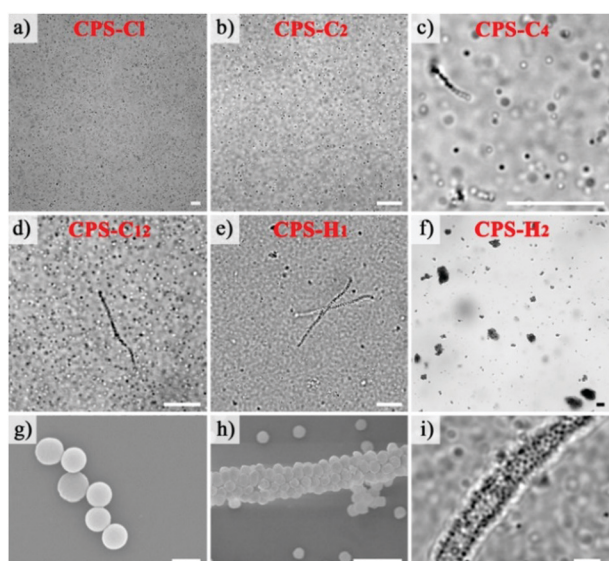


**Fig. 2** Optical micrographs of (a) CPS-Cl, (b) CPS-C<sub>2</sub>, (c) CPS-C<sub>4</sub>, (d) CPS-C<sub>12</sub>, (e) CPS-H<sub>1</sub> and (f) CPS-H<sub>2</sub> dispersed in Milli-Q water. SEM images of (g) a colloidal string, (h) a Bernal spiral-like assembly, (i) Optical micrograph of a tubular assembly. The samples for SEM were freeze-dried to preserve the solution state cluster morphology. Scale bars: 10  $\mu$ m for panels (a–f), 500 nm for panel g, 2  $\mu$ m for panel h and 5  $\mu$ m for panel i.

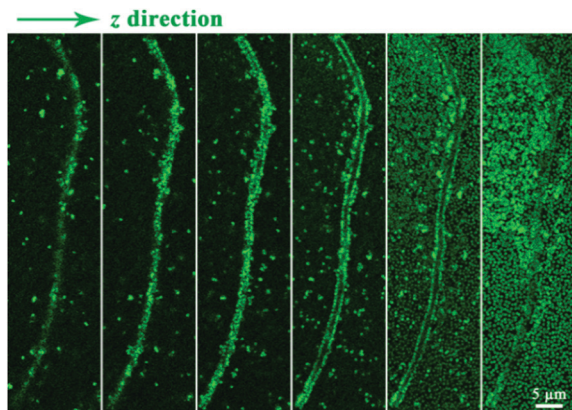


Fig. 3 Confocal microscopy z-stack of tubular assemblies of CPS-H<sub>1</sub>. The z-axis points perpendicular to the imaging plane. Scale bars: 5 μm.

CPS-H<sub>2</sub>, the centrifugation step did not alter the outcome of the assembly process. However, for CPS-H<sub>1</sub>, Bernal spiral-like clusters coexisted with tubular assemblies (2 per 10<sup>8</sup> colloids) after centrifugation (Scheme 1 and Fig. 2i). These tubular superstructures are relatively polydisperse both in their diameter (2–4 μm) and length (20–100 μm) (Fig. S4, ESI<sup>†</sup>), but remained intact equilibration for at least one week, indicating a high structural stability. To elucidate the internal structure of the tubular aggregates, fluorescein sodium salt was added into the centrifuged dispersion. The highly apolar nature of the dye ensures that the hydrophobic surfaces of the particles are fluorescently labeled. This labeling enabled 3D imaging using confocal microscopy (Fig. 3), revealing that the tubular structures are in fact hollow cylinders.

These tubular structures are not predicted by any theoretical or simulation study and present therefore a new cluster morphology for isotropic colloids that interact with each other *via* a combination of short-range attraction and relatively longer-ranged repulsion. Based on previous reports on colloidal assembly of shell-like structures aided by centrifugation we speculate that the shear forces induced by centrifugation play an essential role in the formation of the hollow tubular structures.<sup>3</sup> A detailed study into the formation mechanism of these colloidal tubes is part of future investigation.

In conclusion, we experimentally demonstrate that elongated aggregates of spherical, isotropic colloidal particles can be formed in aqueous environments by the combination of short-range hydrophobic attractions and relatively longer-range electrostatic repulsions. Besides previously predicted and observed Bernal spiral-like assemblies, two additional cluster morphologies were found, namely colloidal strings and hollow tubular assemblies. Our findings enrich the accessible superstructure morphologies

based on simple isotropic colloidal building blocks and provide experimental input for the next generation of theoretical/simulation studies on the intriguing phase behavior of colloids which interact with each other *via* potentials comprised of competing contributions.

Y. Guo is supported by Chinese Scholarship council (File No. 201306200056). Kanvaly Lacina, Hans Meeldijk and Chris Schneijdenberg, Joeri Opdam are thanked for SEM analysis, assisting with freeze-drying, and for drawing the schematic representation of the colloidal tubes, respectively.

## Conflicts of interest

There are no conflicts to declare.

## Notes and references

- (a) O. D. Velev and S. Gupta, *Adv. Mater.*, 2009, **21**, 1897; (b) F. Li, D. P. Josephson and A. Stein, *Angew. Chem., Int. Ed.*, 2011, **50**, 360; (c) L. Xu, W. Ma, L. Wang, C. Xu, H. Kuang and N. A. Kotov, *Chem. Soc. Rev.*, 2013, **42**, 3114; (d) X. Ye and L. Qi, *Nano Today*, 2011, **6**, 608; (e) V. J. Anderson and H. N. W. Lekkerkerker, *Nature*, 2002, **416**, 811; (f) U. Gasser, E. R. Weeks, A. Schofield, P. N. Pusey and D. A. Weitz, *Science*, 2001, **292**, 258.
- (a) D. J. Kraft, R. Ni, F. Smallenburg, M. Hermes, K. Yoon, D. A. Weitz, A. van Blaaderen, J. Groenewold, M. Dijkstra and W. K. Kegels, *Proc. Natl. Acad. Sci. U. S. A.*, 2012, **109**, 10787; (b) B. G. P. van Ravensteijn and W. K. Kegels, *Polym. Chem.*, 2016, **7**, 2858.
- C. H. J. Evers, J. A. Luiken, P. G. Bolhuis and W. K. Kegels, *Nature*, 2016, **534**, 364.
- Z. Tang, Z. Zhang, Y. Wang, S. C. Glotzer and N. A. Kotov, *Science*, 2006, **314**, 274.
- Q. Chen, S. C. Bae and S. Granick, *Nature*, 2011, **469**, 381.
- Q. Chen, J. K. Whitmer, S. Jiang, S. C. Bae and S. Granick Luitjen, *Science*, 2011, **331**, 199.
- Y. Wang, Y. Wang, D. R. Breed, V. N. Manoharan, L. Feng, A. D. Hollingsworth, M. Weck and D. J. Pine, *Nature*, 2012, **491**, 51.
- (a) H. Zhang and D. Wang, *Angew. Chem.*, 2008, **120**, 4048; (b) M. S. Nikolic, C. Olsson, A. Salcher, A. Kornowski, A. Rank, R. Schubert, A. Fromsdorf, H. Weller and S. Forster, *Angew. Chem., Int. Ed.*, 2009, **48**, 2752; (c) H. Wang, L. Chen, X. Shen, L. Zhu, J. He and H. Chen, *Angew. Chem., Int. Ed.*, 2012, **51**, 8021.
- (a) K. Butter, P. H. H. Bomans, P. M. Frederik, G. J. Vroege and A. P. Philipse, *Nat. Mater.*, 2003, **2**, 88; (b) Z. Tang, N. A. Kotov and M. Giersig, *Science*, 2002, **297**, 237.
- J. Groenewold and W. K. Kegels, *J. Phys. Chem. B*, 2001, **105**, 11702.
- (a) F. Sciortino, P. Tartaglia and E. Zaccarelli, *J. Phys. Chem. B*, 2005, **109**, 21942; (b) D. Banerjee, B. A. Lindquist, R. B. Jadrich and T. M. Truskett, *J. Chem. Phys.*, 2019, **150**, 124903.
- (a) A. I. Campbell, V. J. Anderson, J. S. van Duijneveldt and P. Bartlett, *Phys. Rev. Lett.*, 2005, **94**, 208301; (b) S. Mossa, F. Sciortino, P. Tartaglia and E. Zaccarelli, *Langmuir*, 2004, **20**, 10756; (c) T. H. Zhang, J. Klok, H. R. Tromp, J. Groenewold and W. K. Kegels, *Soft Matter*, 2012, **8**, 667.
- M. Weijers, R. W. Visschers and T. Nicolai, *Macromolecules*, 2002, **35**, 4753.
- B. G. P. van Ravensteijn and W. K. Kegels, *Langmuir*, 2014, **30**, 10590.
- B. G. P. van Ravensteijn, M. Kamp, A. van Blaaderen and W. K. Kegels, *Chem. Mater.*, 2013, **25**, 4348.